RESEARCH PAPER

Acta Neurobiol Exp 2023, 83: 317–330
DOI: 10.55782/ane-2023-2437

Hydrogen-rich saline promotes neuronal recovery in mice with cerebral ischemia through the AMPK/mTOR signal-mediated autophagy pathway

Jing Wang[1,2], Xiang-jian Zhang[1,2]*, Yuan-yuan Du[1,2], Guang Shi[1,2], Cong-Cong Zhang[1,2], Rong Chen[1,2]

[1] Department of Neurology, Second Hospital of Hebei Medical University, Shijiazhuang, Hebei, China,
[2] Hebei Key Laboratory of Vascular Homeostasis and Hebei Collaborative Innovation Center for Cardio-cerebrovascular Disease, Shijiazhuang, Hebei, China,
** Email: zhang6xj@aliyun.com*

This study explored the protective effect and mechanism of hydrogen-rich saline (HRS) on the neurological function of mice with cerebral ischemia. Effects of HRS on neurological function in mice with cerebral ischemia were evaluated by neurological function scores. Infarct volume and histological damage were evaluated by 2,3,5-triphenyl tetrazolium chloride staining (TTC staining). Golgi-Cox staining was conducted to measure the morphological changes of neuronal dendrites and dendritic spines. The expression of neuronal markers was detected by immunofluorescence. Western blot was used to detect protein expression. The infarct volume of mice in the HRS-H group decreased significantly compared to that of the distal middle cerebral artery occlusion (dMCAO) group. Mice in the HRS-H group had a lower neurological deficit score than that in the dMCAO group. Compared to the dMCAO group, the activity of superoxide dismutase (SOD) and the level of glutathione (GSH) significantly increased in the HRS-H group. Compared with the dMCAO group, the number of apoptotic cells in the HRS-H group decreased. Administration of HRS was shown to be able to decrease cavitation of the brain cortex after ischemia. The spine density in the HRS-H group increased compared to that of the dMCAO group. In the *in vitro* experiment, compared with the oxygen-glucose deprivation (OGD) group, the active oxygen content in the 75% HRM group decreased, and the mitochondrial membrane potential and adenosine triphosphate (ATP) content increased. Compared with the OGD group, the ratio of P-AMPK and the levels of LC3II/LC3I in the hydrogen-rich medium (HRM) group was upregulated, and P-mTOR levels and P62 levels in the HRM group were down-regulated. HRS can enhance neuroplasticity after ischemia and promote neurological recovery in mice with cerebral ischemia, which may involve the autophagy pathway mediated by the AMPK/mTOR signaling pathway.

Key words: hydrogen-rich saline, cerebral ischemia, neuronal function, stroke, signaling

INTRODUCTION

Stroke is the leading cause of lifelong disability, of which ischemia accounts for the majority, with a rising incidence worldwide (Sennfält et al., 2021). Neuronal cell damage during cerebral ischemia or stroke is a serious neurological complication that limits survival and/or functional recovery (Fu et al., 2022). The brain immediately initiates self-defense, including anti-oxidative stress, anti-inflammation and anti-apoptosis, and self-repair mechanisms, including vascular plasticity and neuroplasticity after the onset of cerebral ischemia (Williamson et al., 2020; Joy and Carmichael, 2021), to mitigate neurologic impairment. However, neurological damage to the adult central nervous system of mammals commonly produces persistent deficits with limited recovery of function. At present, common treatments for stroke include intravenous thrombolytics, tissue plasminogen activator (tPA), and endovascular treatment (Yousefifard et al., 2020). In addition, only a minority of patients with acute ischemic stroke are eligible for revascularization therapies (van

Received 23 March 2023, accepted 18 July 2023

der Worp et al., 2019). Neurological recovery therapy based on neuroplasticity plays a critical role in functional recovery after cerebral ischemia (Zhang et al., 2019). Since most patients with cerebral ischemia are left with neurological dysfunction, it is urgently necessary to explore effective drugs for the treatment of cerebral ischemia.

Neuronal necrosis or apoptosis is the leading cause of loss of neuronal function since neurons are the executors of neural activity (Moujalled and Liddell, 2021). Rescue neurons in ischemic penumbra and rehabilitation neural circuitry are helpful in the recovery of neurological function. Accumulated studies indicate that scavenging oxidative stress contributes to reducing neuronal apoptosis in ischemic penumbra, and synaptic remodeling contributes to long-term neurological recovery (Xu et al., 2020; Yan et al., 2020). In addition, autophagy inhibited by the AMPK-mTOR signaling pathway also has a protective effect on oxygen-glucose deprivation/re-oxygenation (OGD/R)-induced neuronal damage (Gong et al., 2021).

Hydrogen, as a novel medical gas, has been demonstrated to exert a therapeutic effect in preclinical and clinical studies. Ono et al. (2011, 2017) confirmed that hydrogen inhalation could improve magnetic resonance imaging (MRI) and neurological function in patients with acute cerebral infarction in clinical studies, which suggests the important role of hydrogen in neuronal recovery; however, the detailed underlying mechanisms remain to be studied. Hydrogen alleviates neurological deficits in neonatal hypoxic-ischemic encephalopathy by reducing phagocytosis in microglia and modulating apoptosis in neurons (Ke et al., 2020; Wang et al., 2020). Hydrogen exerts protective effects in cerebral ischemia/reperfusion animals *via* anti-oxidative stress and anti-inflammatory and anti-apoptosis mechanisms (Ohsawa et al., 2007; Huang et al., 2019; Mo et al., 2019). A study by Bai et al. (2016) found that HRS exerts neuroprotection against hypoxia-ischemia in neonatal mice by mediating endoplasmic reticulum stress and autophagic machinery. However, relatively little is known regarding the potential for HRS to restore cerebral ischemia-induced behavioral deficits and whether such effects might involve antioxidant action and mediation of synapse remodeling.

In this study, the protective effect of and mechanism of HRS in the neurological function of mice with cerebral ischemia were studied in vivo and in vitro using the distal dMCAO mouse model, and the effect of HRS on cerebral ischemia in mice was evaluated. It provides theoretical support for the clinical development of drugs for the treatment of cerebral ischemia and stroke.

METHODS

Animals

Male C57BL/6 mice (8–12 weeks, 22–25 g) and pregnant mice (gestation 15–18 days) were used and obtained from Vital River Corporation (Beijing, China). All mice were group-housed under specific conditions with a controlled temperature (20–25°C), controlled humidity (55–65%) and a fixed 12/12 hour light/dark cycle. They were allowed to access food and water ad libitum. All experiments were approved by the Institutional Animal Care and Management Committee of the Second Hospital of Hebei Medical University and conducted in compliance with the Guide for the Care and Use of Laboratory Animals. All efforts were made to maximally relieve animal suffering. See the additional flowchart.

Establishment of the distal middle cerebral artery occlusion (dMCAO) mouse model

The cerebral ischemia injury animal model was established by dMCAO surgery, as previously reported (Llovera et al., 2014). In short, animals were anesthetized with isoflurane (5% for induction and 1.5%–0.5% for maintenance). Then, a median incision was made in the neck; the right common carotid artery (CCA), internal carotid artery (ICA), and external carotid artery (ECA) were gently isolated. CCA was completely exposed and ligated with a suture permanently. The MCA located between the right eye and the right ear was coagulated carefully without brain tissue damage. The incisions were sutured after determining the absence of blood flow in the distal MCA. The body temperature of the mouse was maintained at 37.0 ± 0.5°C during surgery by a thermostatic pad. Mice in the sham group had the same surgery except for ligation and electrocoagulation.

HRS and HRM preparation

HRS and HRM were prepared according to previously described methods (Song et al., 2015). Briefly, hydrogen gas was dissolved in saline or normal medium for two h under 0.4 MPa until reaching saturation using a hydrogen-rich-solution-producing apparatus. The final concentration of hydrogen was maintained at 1.2 ppm – 1.4 ppm, measured by a dissolved hydrogen indicator (MiZ Cor. Japan).

Groups and drug treatment

260 mice (including 24 pregnant mice) were randomly divided into five groups using a completely randomized design. Briefly, the mice were first numbered and then randomly assigned into the sham group: mice received an equal volume of vehicle (0.9% saline solution), the dMCAO group: mice received an equal volume of vehicle, the HRS-L group: dMCAO mice received 5 ml/kg HRS, the HRS-M group: dMCAO mice received 10 ml/kg HRS, and the HRS-H group: dMCAO mice received 20 ml/kg HRS. Mice in the sham group were subjected to sham surgery, and mice in other groups underwent dMCAO surgery.

Neurobehavioral tests

To determine whether HRS has a therapeutic effect on mice with cerebral ischemia, a series of neurobehavioral tests were performed, including a modified neurological severity score test (mNSS test), rotarod test, corner test, and adhesive removal test, which were conducted by an investigator blinded to the treatment groups.

mNSS test

The mNSS is a composite of motor, sensory, reflex, and balance tests, grading on a scale ranging from 0 to 18 (normal score, 0; maximal deficit score, 18). The subject would get one score when it lacked a tested reflex and was incapable of accomplishing the test. Higher scores indicated more severe neurological deficits.

Rotarod test

The rotarod test was conducted to evaluate motor function (Zhang et al., 2021). Mice were selected for inclusion if they were able to remain on the rod (4 rpm) for more than 100s after being trained three times a day, at 15-minute intervals, for three days. For the test, mice were placed on an accelerating rotating rod (from 4 to 40 rpm in 4 min) 3 times a day, with a 15-minute interval. The time until the mouse fell off the rod, a maximum of 240 s, was recorded, and a low average indicated severe locomotion impairment.

Corner test

The corner test was used to estimate sensorimotor ability, as described previously (Xue et al., 2019). Before the dMCAO operation, mice were exposed to 10 trials a day, excluding those with 80–100% asymmetric turns. For the test, all mice underwent ten trials, each for 30 s, and the number of right turns was recorded. The more times the mouse turned to the right, the more severe the sensorimotor disability was.

Adhesive removal test

The adhesive removal test was conducted to examine motor and sensory functions. Mice were pre-trained once a day for five days in a prepared clear white cage, and the mice that could remove the tape within 20 s were selected. For the test, the contact time (the period that the mouse detects the adhesive strips) and removal time (the period that the mouse removes the adhesive strips, maximum of 120 s) were recorded, respectively, three times a day, and the average was taken as the test data.

TTC staining

TTC staining was performed to define the infarct volume. Mice were sacrificed at a scheduled time, and coronal sections at 1 mm intervals were completely immersed into 2% TTC solution and incubated for 20 min at 37 . After fixation with 4% paraformaldehyde (PFA) for 24 h, the images of the brain slices were captured by a digital camera. The infarct volume was measured by ImageJ and calculated with the corrected equation: (infarct volumes)% = [total infarct volume – (ipsilateral hemisphere volume – contralateral hemisphere volume)] / contralateral hemisphere volume × 100%.

Cortical width index (CWI)

The CWI was applied to determine histological damage in the long-term ischemic brain. After being perfused with 4% PFA, the whole brain was dissected and captured with a digital camera. The contralateral width (the length from the midpoint of the forebrain midline to the lateral edge) and the ipsilateral width the length from the midpoint of the forebrain midline to the edge of cortical cavitation were evaluated with ImageJ software (NIH, USA). CWI = the ipsilateral width / the contralateral width.

Golgi-Cox staining

Golgi-Cox staining was conducted to measure morphological changes in neuronal dendrites and dendritic spines. The experimental procedure was carried out following the manufacturer's instructions (Hito-Cox

OptimStain Kit). It is worth pointing out that the thickness of the brain slices was 150 μm as it has been shown that the effects of ischemia are limited to neurons close to the infarct border (<200 μm). Fully-impregnated neurons located in the ischemic penumbra were selected as long as they had little intersection with other components. The selected dendrites were not truncated in the plane of the slice. Images were captured using a light microscope under 10X and oil-100X and were quantified using ImageJ.

Primary cortical neuron culture

Culturing of primary cortical neurons (PCNs) was carried out, as mentioned previously (Xu et al., 2012). Briefly, a sample of the cerebral cortex was taken from a C57BL/6 fetus at embryonic day 16–18, and the meningeal tissue was isolated carefully. The minced cortex was digested sequentially with solutions of papain (2 mg/ml) for 30 min and DNase I (200 μl, 2.5 mg/ml) for 2 min at 37°C, and then terminated with planting medium (DMEM/F12 containing 10% fetal bovine serum and 1% penicillin/streptomycin) for 2 min twice. The supernatant was collected, and the brain fractions were triturated gently about ten times with a Pasteur pipette to dissociate into single neurons in 3 ml of planting medium three times and filtered through 40 μm-diameter sieves. After counting the population, neurons were seeded on plates covered with poly-D-lysine (0.1 mg/ml) at 5×10^5 cells/ml or 1×10^6 cells/cm^2. 4–6 h after plating, culturing medium (Neurobasal medium containing 2% B27, 1% L-Glutamine and 1% penicillin/streptomycin) was replaced and renewed in half every 2–3 d to 7 days.

OGD

PCNs were submitted to oxygen-glucose deprivation (OGD) to mimic cerebra ischemia in vitro. PCNs were rinsed with DMEM/F12 once and incubated with glucose-free medium in a hypoxic incubator (94% N2, 5% CO2, 1% O2) for a scheduled time. Thereafter, the medium of the OGD group was renewed with culturing medium or treated with a different HRM medium. The control group was incubated in culturing medium in a normal incubator (21% O2, 5% CO2).

Cell viability assay

The cell viability rate was assayed using the Cell Counting Kit-8 (CCK-8, Dojindo, Japan). The cells were seeded in 96-well plates at a density of 2×10^5/ml and cultured for seven days. After treatment with OGD, 10 μl of CCK-8 was added to the 96-well plates and then incubated at 37°C for 2 h. The absorbance value at 450 nm was measured using a microplate reader (TECAN). Cell viability of the treatment groups was expressed as the percentage of viable cells normalized to that of the control group. Five replicated wells were set up in each group. The results shown were representative of three independent experiments.

The detection of cell ROS, JC-1 and ATP

PCNs were planted in a 96-well plate (1×10^5/cm^2), a 24-well plate (1×10^5/cm^2), and a 6-well plate (2×10^5/cm^2), cultured for seven days and then underwent 5 hours of OGD. Six hours after OGD, intracellular ROS levels, mitochondrial membrane potential and ATP were quantified by a reactive oxygen species assay kit (Nanjing Jiancheng, China), JC-1 assay kit (Beyotime, China) and ATP assay kit (Beyotime, China), respectively.

SOD, GSH and MDA (malondialdehyde) detection

After treating dMCAO for 24 h, a portion of the brain tissue was homogenized in physiological saline (0.1 mL/100 g) and then centrifuged at 15,000 g for 15 minutes. The clear upper supernatants were collected for analyzing oxidative stress (MDA, SOD and GSH). According to the manufacturer's instructions (Jiancheng, Nanjing, China), the MDA, SOD and GSH concentrations were measured by MDA, SOD and GSH ELISA kits, respectively.

Immunofluorescence staining

Anesthetized mice were fixed by transcardial perfusion with cold 0.9% saline and 4% PFA continuously. Coronal slices of frozen brain (15-μm thick) were sectioned using a cryostat microtome cryotome (Thermo Scientific, USA). At the start, the slices were washed with 0.01M PBS three times for 5min each time and then permeabilized with 0.3% Triton X-100 for 15 min. After being blocked with 10% donkey serum for 60 min at 37°C, the slices were incubated with primary antibodies overnight at 4°C (at least 16 hour-incubation). On the second day, the slices were washed with 0.01 M PBS three times for 5 min each time and incubated with corresponding specific second antibodies (Alexa Fluor 488, Jackson Immuno Research Labs) for 60 min at room temperature. Finally, the slices were washed again as

above and sealed with DAPI Fluoromount-G (Southern Biotech, USA), which counterstained the cell nuclei. Immunofluorescence images were recorded using a laser scanning confocal microscope (Zeiss LSM880, German) and measured using ImageJ software.

Western blotting

Total protein was extracted from the brain cortex with a total protein extraction solution (Applygen, China) and PCNs using a radioimmunoprecipitation assay (RIPA) lysis buffer (Solarbio, China) containing 1% protease inhibitor cocktail (Sigma, USA) and 1% phosphatase inhibitor (Applygen, China); the concentration was evaluated with a BCA protein assay kit (Thermo Scientific, USA). Then, total protein of equivalent amounts (50 μg) was divided by SDS-PAGE and fully transferred to a PVDF (polyvinylidene fluoride) membrane. After being blocked with 5% BAS (Woosen, China) for 60 min at temperature, the membranes were incubated with primary antibodies overnight at 4°C, including PSD 95, SYP, AMPK, P-AMPK, mTOR, P-mTOR, P62, LC3, and GAPDH. After an at least 16 hour-incubation of the membrane, the membrane was washed with 1 × TBST three times for 5 min each time and incubated with corresponding specific second antibodies (Goat Anti-Rabbit IgG (H&L) Antibody DyLight 800 Conjugated, 1:10000, Rockland; Goat Anti-Mouse IgG, Dylight 680, 1:2000, Abbkine) for 60 min at room temperature. Finally, the membranes were washed again, as described above, and the images were captured using an Odyssey infrared scanner (LICOR Bioscience, Lincoln, NE, USA) and analyzed by ImageJ software.

Statistical analysis

The data are presented as mean ± SEM and were analyzed using SPSS 21.0 statistic software (SPSS for Windows 21.0). The LSD-T test was used for intergroup comparisons, and nonparametric test methods were used for incomplete variance and in the case of not meeting the normal distribution. $p<0.05$ was considered statistically significant.

RESULTS

HRS reduced infarct volume and improved neurological function after MCAO

To determine whether HRS had neuroprotective effects in acute ischemic stroke, TTC staining and the mNSS and rotarod test were carried out 24 h after dMCAO. Compared with the dMCAO group, the infarct volume was smaller in the HRS-L group and HRS-M group 24 h after surgery, but the difference was not statistically significant ($p>0.05$). However, infarct volume in the HRS-H group significantly decreased compared to that of the dMCAO group ($F_{(3,16)}=15.147$, $p<0.001$) (Fig. 1A and B). Additionally, mice in the HRS-H group had a lower neurological deficit score than those in the dMCAO group ($H_{(3)}=14.028$, $p<0.01$) (Fig. 1C). In line with this, the HRS-H group displayed better neurofunction in the motor and balance skills than the dMCAO group ($F_{(3,36)}=4.282$, $p<0.05$) (Fig. 1D). These data collectively served to assess the neuroprotective effects of HRS against acute ischemic brain damage.

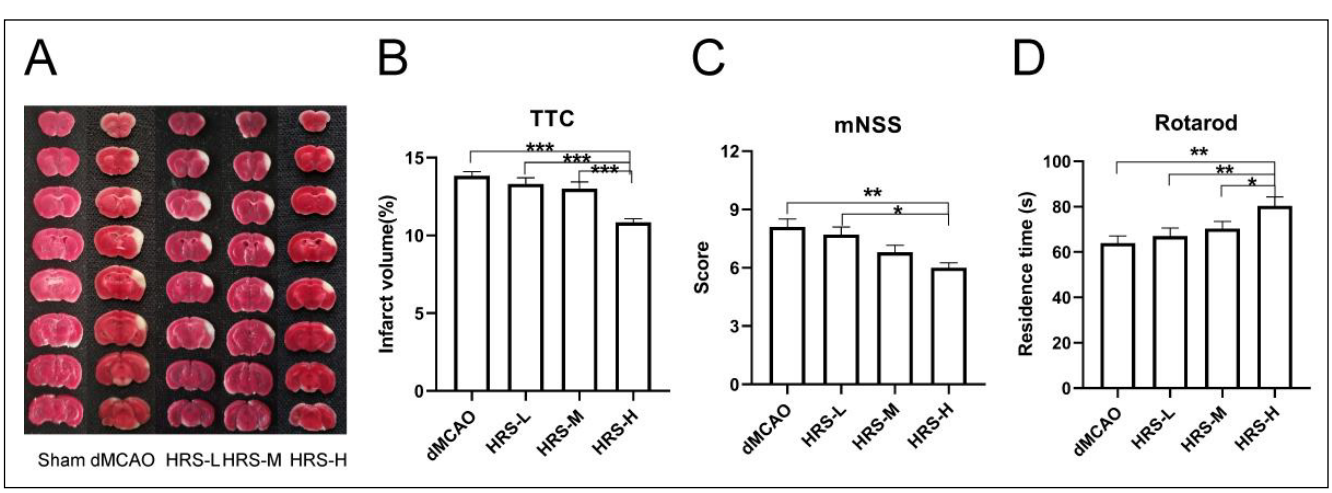

Fig. 1. HRS reduced infarct volume and improved neurologic function after dMCAO. (A) Representative TTC-stained sections in the Sham group, dMCAO group and HRS group 24 h after stroke. (B) Effect of HRS on infarct volume 24 h after stroke. (C) The mNSS evaluation 24 h after dMCAO. (D) Rotarod test evaluation in the dMCAO group, HRS-L group, HRS-M group and HRS -H group 24 h after dMCAO. *$p<0.05$, **$p<0.01$, ***$p<0.001$.

HRS alleviated ischemia-induced oxidative stress and neuronal apoptosis in penumbra during acute cerebral ischemia

To assess the effect of HRS on oxidative stress in dMCAO mice, MDA, GSH and the activity of SOD in the cerebral penumbra were measured 24 h after ischemia. Compared to the dMCAO group, the HRS-H group had a significant increase in SOD activity ($F_{(2,15)}$=13.895, p<0.05) and GSH level ($F_{(2,15)}$=23.430, p<0.05), indicating its antioxidant ability, and a decrease in MDA content ($F_{(2,15)}$=25.642, p<0.05), indicating a reduction in oxidative stress (Fig. 2E-G). To further investigate the impact of HRS on the mice in acute ischemia, we evaluated the population of neurons at 24 h after dMCAO by immunofluorescence staining. The results showed that the morphology of neurons in the dMCAO mouse penumbra had shrunk, and the number was significantly decreased compared to mice in the Sham group and HRS-H group ($F_{(2,78)}$=39.235, p<0.01) (Fig. 2A and 2B). In addition, compared with the Sham group, the number of apoptotic cells in the dMCAO group was significantly higher ($H_{(2)}$=68.911, p<0.001) (Fig. 2D). Compared with the dMCAO group, the number of apoptotic cells in the HRS-H group decreased, and the difference was statistically significant (p<0.001) (Fig. 2C and 2D). Therefore, treatment with HRS-H could have protected the neurons by reducing oxidative stress and apoptosis, which is consistent with previous behavioral tests.

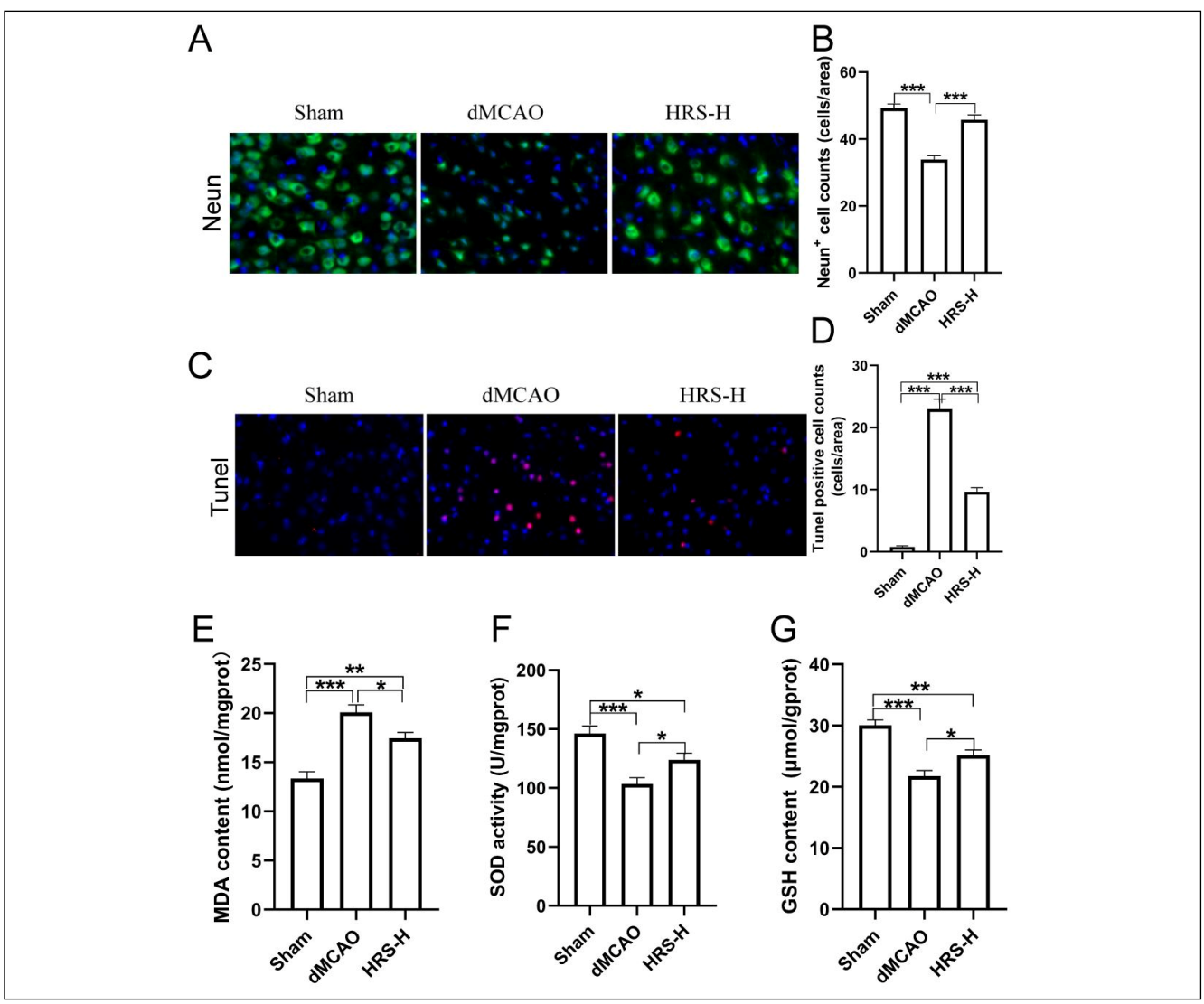

Fig. 2. HRS alleviated ischemia-induced oxidative stress and neuronal apoptosis in penumbra during acute cerebral ischemia. (A) Immunofluorescence images of NeuN (green) and DAPI (blue) staining. (B) The counts of NeuN + cells. (C) TUNEL fluorescence detection of apoptosis. (D) The counts of TUNEL-positive cells. (E) Detection of MDA content. (F) Detection of SOD activity. (G) Detection of GSF content. *p<0.05, **p<0.01, ***p<0.001.

HRS promoted long-term neurologic recovery after ischemia

We investigated the effects of long-term HRS administration on infarct volume 14 days post-ischemia and observed a significant reduction in infarct volume in the HRS-H group compared to the dMCAO group ($t_{(2)}$=2.662, p<0.05) (Fig. 3A and 3C). CWI results revealed that the administration of HRS could decrease cavitation of the brain cortex compared to the administration of saline at 14 days after ischemia (Z=-2.722, p<0.05) (Fig. 3B and 3D). Neurobehavioral tests, such as the rotarod, corner, and adhesive removal tests, were performed from day 1 to day 14 days post-dMCAO to evaluate HRS treatment efficacy during later stages of ischemia. In the rotarod test, all mice displayed a decrease in staying time compared to their scores pre-operation. Mice treated with HRS-H exhibited an increase in staying time compared to the dMCAO mice at day 1 ($t_{(18)}$=-3.215, p<0.01), day 7 ($t_{(18)}$=-2.704, p<0.05), day 14 ($t_{(18)}$=-2.668, p<0.05), day 21 ($t_{(18)}$=-3.012, p<0.01) and day 28 ($t_{(18)}$=-2.628, p<0.05), respectively (Fig. 3E). In the corner test, all mice showed asymmetric behavior after ischemia. And there was a significant decrease in number of right turns between the HRS-H group and the dMCAO group at day 1 ($t_{(18)}$=2.377, p<0.05), day 7 ($t_{(18)}$=2.331, p<0.05), and day 14 ($t_{(18)}$=2.611, p<0.05) (Fig. 3F). In the adhesive removal test, contact time and removal time of the paralyzed forelimb were prolonged compared to their pre-operation test (Fig. 3G and H). HRS-H treatment markedly reduced the contact time and removal time of the impaired limb 14 days after cerebral infarction (Fig. 3G and 3H). Collectively, our results suggest that HRS can enhance neurological recovery following ischemia.

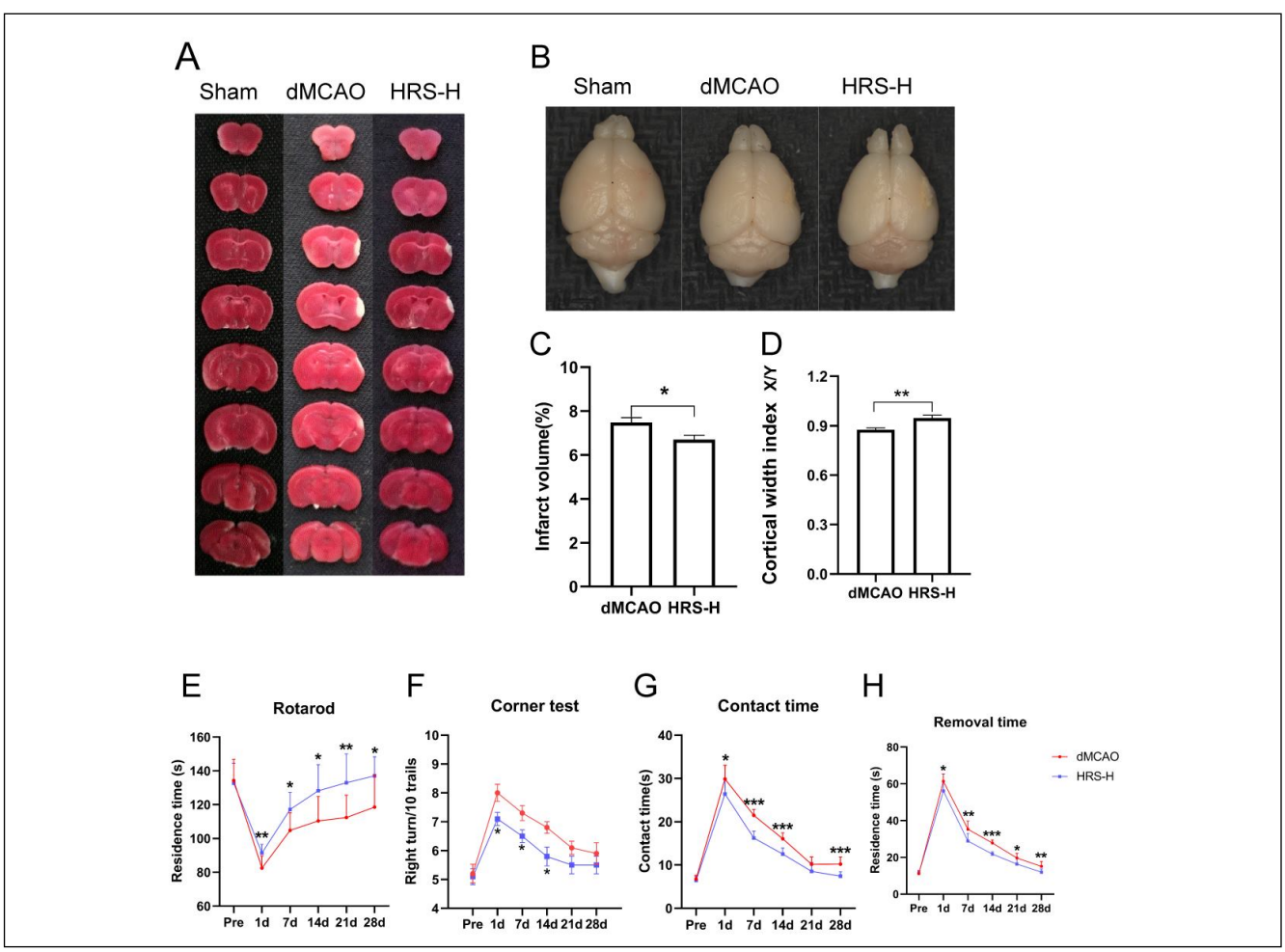

Fig. 3. HRS promoted long-term neurological recovery after ischemia. (A) Representative TTC-stained sections in the Sham group, dMCAO group and HRS group 14 d after stroke. (B) Effect of HRS on infarct volume 14 d after stroke. (C) Image of the cerebral cortex. (D) Cortical width index. (E) Rotarod test evaluation in the dMCAO group and the HRS-H group before operation and 1 d, 7 d, 14 d, 21 d, and 28 d after dMCAO. (F) Corner test evaluation in the dMCAO group and HRS-H group before operation and 1 d, 7 d, 14 d, 21 d, and 28 d after dMCAO. (G–H) Adhesive removal test evaluation in the dMCAO group and HRS-H group before operation and 1 d, 7 d, 14 d, 21 d, and 28 d after dMCAO. *p<0.05, **p<0.01, ***p<0.001.

HRS enhanced long-term neuronal plasticity after ischemia

Golgi-Cox staining was conducted to evaluate spine density and determine the sum of dendritic length and branches on day 14 after ischemia. Morphological analysis was performed on the pyramidal neurons in layer II/III of the motor cortex in the penumbra. Compared to the sham group, spine density and dendritic branches declined in the dMCAO group and HRS-H group (Fig. 4A-D). In the HRS-H group, spine injury was mitigated as the spine density of the HRS-H group showed an increase compared to that of the dMCAO group at day 14 ($H_{(2)}$=198.536, p<0.001) (Fig. 4A and C). Nevertheless, no differences between the dMCAO group and HRS-H group were found in regard to dendritic branches (p>0.05) (Fig. 4D). Furthermore, synapse-related proteins such as PSD95 and SYP were measured by western blot. The results showed that PSD95 ($F_{(2,15)}$=17.158, p<0.05) and SYP ($F_{(2,15)}$=5.005, p<0.01) protein were increased in the HRS-H mice compared with the dMCAO group (Fig. 4E-G). Taken together, HRS was able to ameliorate spine and branch injury in the chronic phase of ischemia.

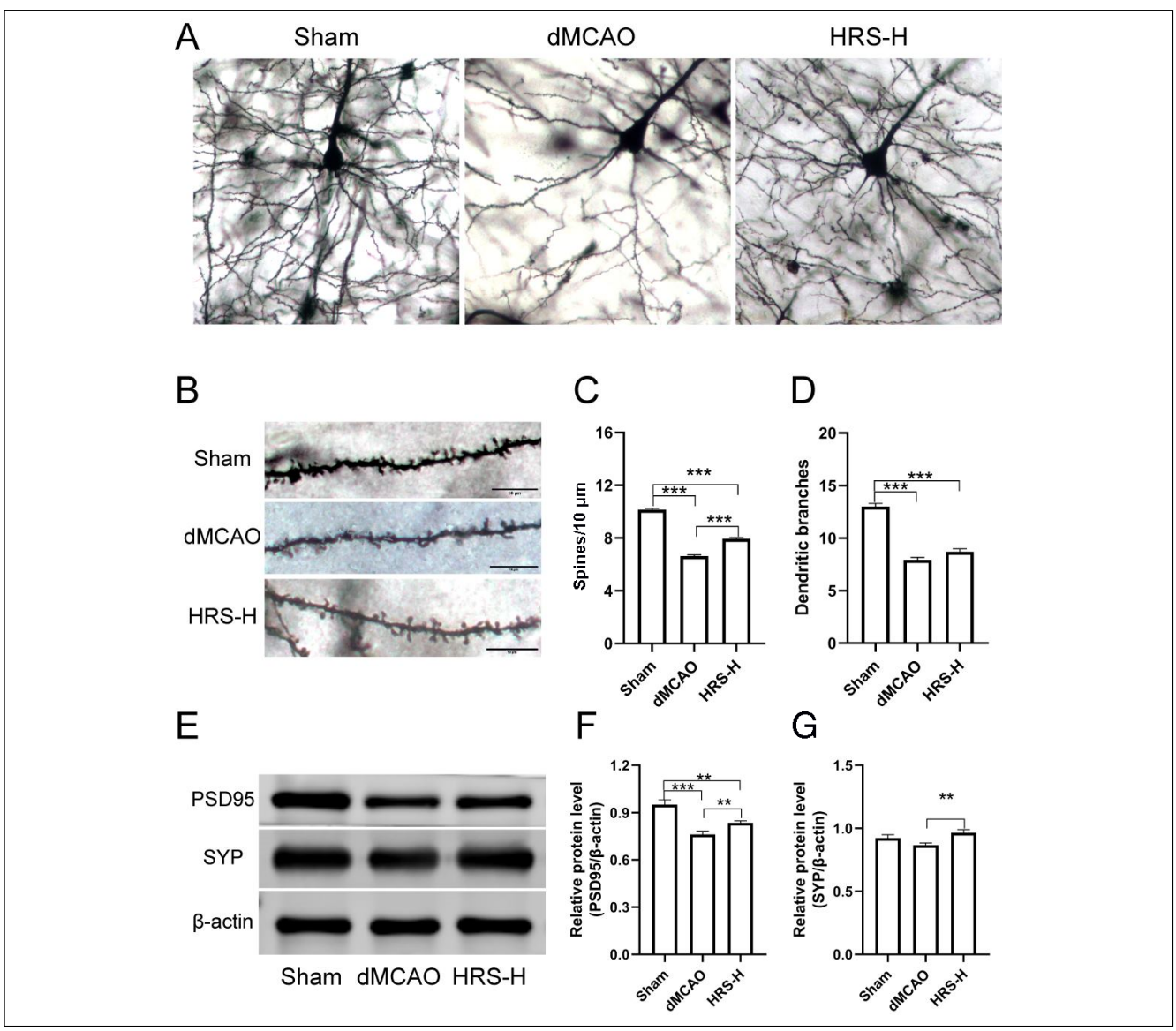

Fig. 4. HRS enhanced long-term neuronal plasticity after ischemia. (A) Image of Golgi-Cox staining in the Sham group, dMCAO group, and HRS-H group 14 d after dMCAO. (B) Spine density of Golgi-Cox staining in the Sham group, dMCAO group and HRS-H group 14 d after dMCAO. (C) The sum of dendritic length in the Sham group, dMCAO group and HRS-H group 14 d after dMCAO. (D) Dendritic branches in the Sham group, dMCAO group, and HRS -H group 14 d after dMCAO. (E–G) The expression of PSD95 and SYP protein was detected by western blot. *p<0.05, **p<0.01, ***p<0.001.

HRM mitigated OGD-induced injury in PCNs

To determine the optimal time for OGD, PCNs were subjected to OGD for different periods, ranging from 1 hour to 6 hours, after being cultured for 7 days in vitro. Following OGD treatment, cell viability was evaluated with a CCK8 kit. A duration of 5 hours of OGD was confirmed to be the appropriate time at which cell viability was induced to decrease by 50% compared to the control group ($H_{(6)}$=39.091, p<0.001) (Fig. 5A). Additionally, the protective effects of HRM were evaluated based on a dosage-curve in PCNs after 5 hours of OGD treatment. Results indicated that applying 75% HRM significantly increased cell viability, and it was used in subsequent experiments ($H_{(5)}$=29.865, p<0.01) (Fig. 5B). Further investigations were carried out to determine the effects of HRM on reactive oxygen species, mitochondrial membrane potential, and ATP content *in vitro*. It was found that relative to the control group, OGD treatment significantly increased ROS content ($F_{(2,15)}$=159.821, p<0.001) and decreased mitochondrial membrane potential and ATP content ($F_{(2,15)}$=66.192, p<0.001) in PCNs (Fig. 5C-E). Compared with the OGD group, the active oxygen content in the 75% HRM group decreased ($F_{(2,15)}$=159.821, p<0.001), and the mitochondrial membrane potential ($F_{(2,15)}$=66.192, p<0.01) and ATP

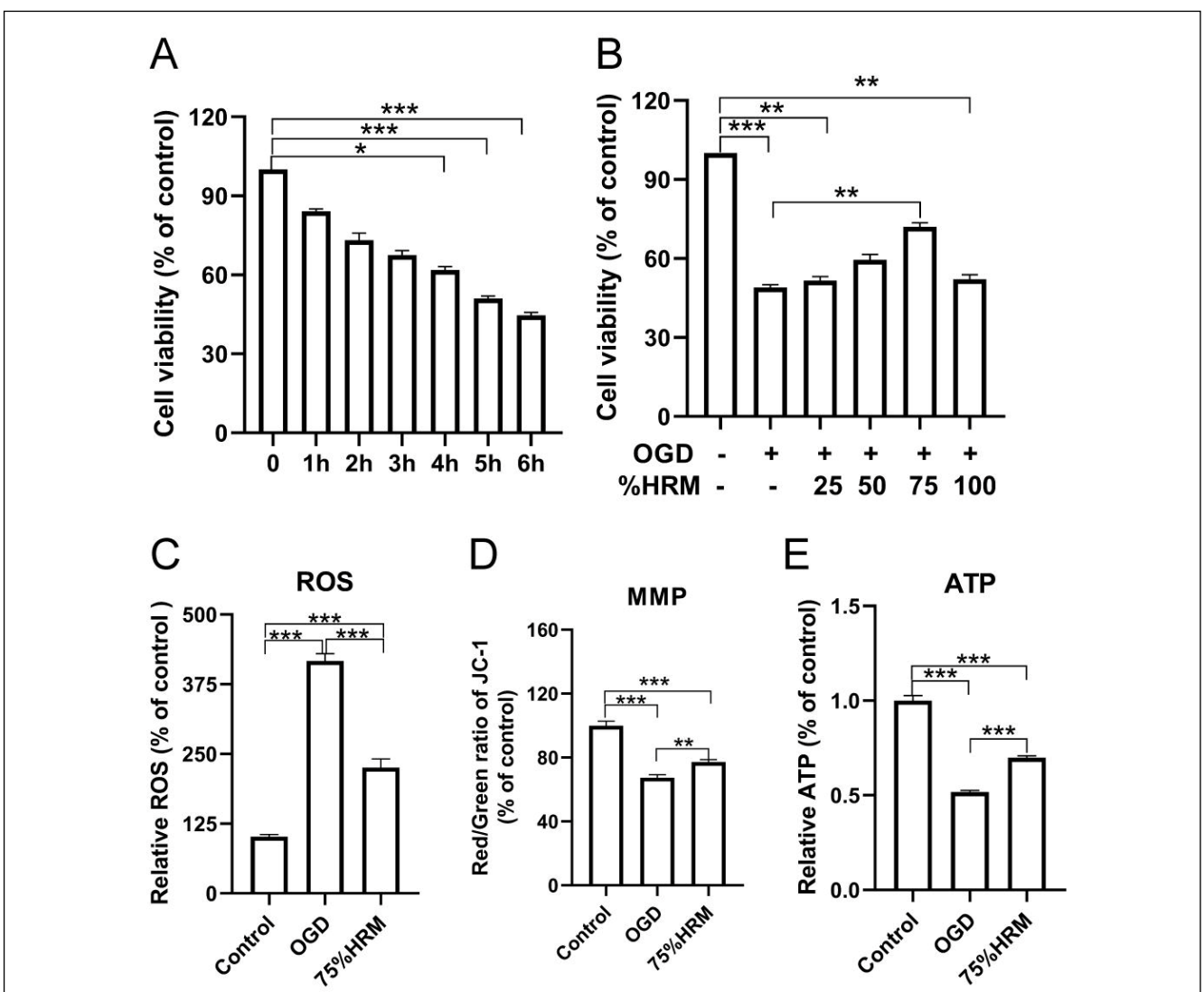

Fig. 5. HRM mitigated OGD-induced injury in PCNs. (A) The effective concentration of HRS for cell viability assessment. (B) Cell viability was measured after OGD treatment at different times. (C) Relative ROS content of mice in the control group, OGD group and 75% HRM group. (D) The mitochondrial membrane potential of mice in the control group, OGD group and 75% HRM group. (E) ATP levels of mice in the control group, OGD group and 75% HRM group. *p<0.05, **p<0.01, ***p<0.001.

content ($F_{(2,15)}$=198.920, p<0.001) increased, and the difference was statistically significant (Fig. 5C–E). These results demonstrated that HRM could alleviate OGD-induced injury in PCNs.

HRM promoted AMPK phosphorylation and autophagy in PCNs after OGD

We further explored the molecular mechanism underlying the protective effects of HRM on PCNs subjected to OGD by western blotting. Given the important role of AMPK in the process of synaptic remodeling, we examined AMPK and its downstream molecules (Gong et al., 2021). The quantified results showed that OGD induced a decrease in the ratio of p-AMPK ($F_{(2,12)}$=9.461, p<0.01), meanwhile p-mTOR, which is downstream of AMPK, increased ($F_{(2,12)}$=10.704, p<0.01) (Fig. 6A–C). Compared with the OGD group, the ratio of p-AMPK in the HRM group was upregulated ($F_{(2,12)}$=9.461, p<0.01), and p-mTOR levels in the HRM group were down-regulated ($F_{(2,12)}$=10.704, p<0.05) (Fig. 6A–C). Moreover, autophagy-related molecules were investigated because they are regulated by AMPK/mTOR and are part of crucial mechanisms involved in neuroprotection and neuroplasticity (Gong et al., 2021). The results showed that OGD decreased the ratio of LC3II/LC3I ($F_{(2,12)}$=10.532, p<0.01) and increased the expression of P62 ($F_{(2,12)}$=4.354, p<0.05) compared to the control group (Fig. 6D–F). Compared with OGD group, the levels of LC3II/LC3I in the HRM group were upregulated ($F_{(2,12)}$=10.532, p<0.01) and the levels of P62 in the HRM group were downregulated ($F_{(2,12)}$=4.354, p<0.05) (Fig. 6D–F). Collectively, the results indicated that hydrogen protected neurons against OGD-induced injury by promoting AMPK/mTOR/autophagy.

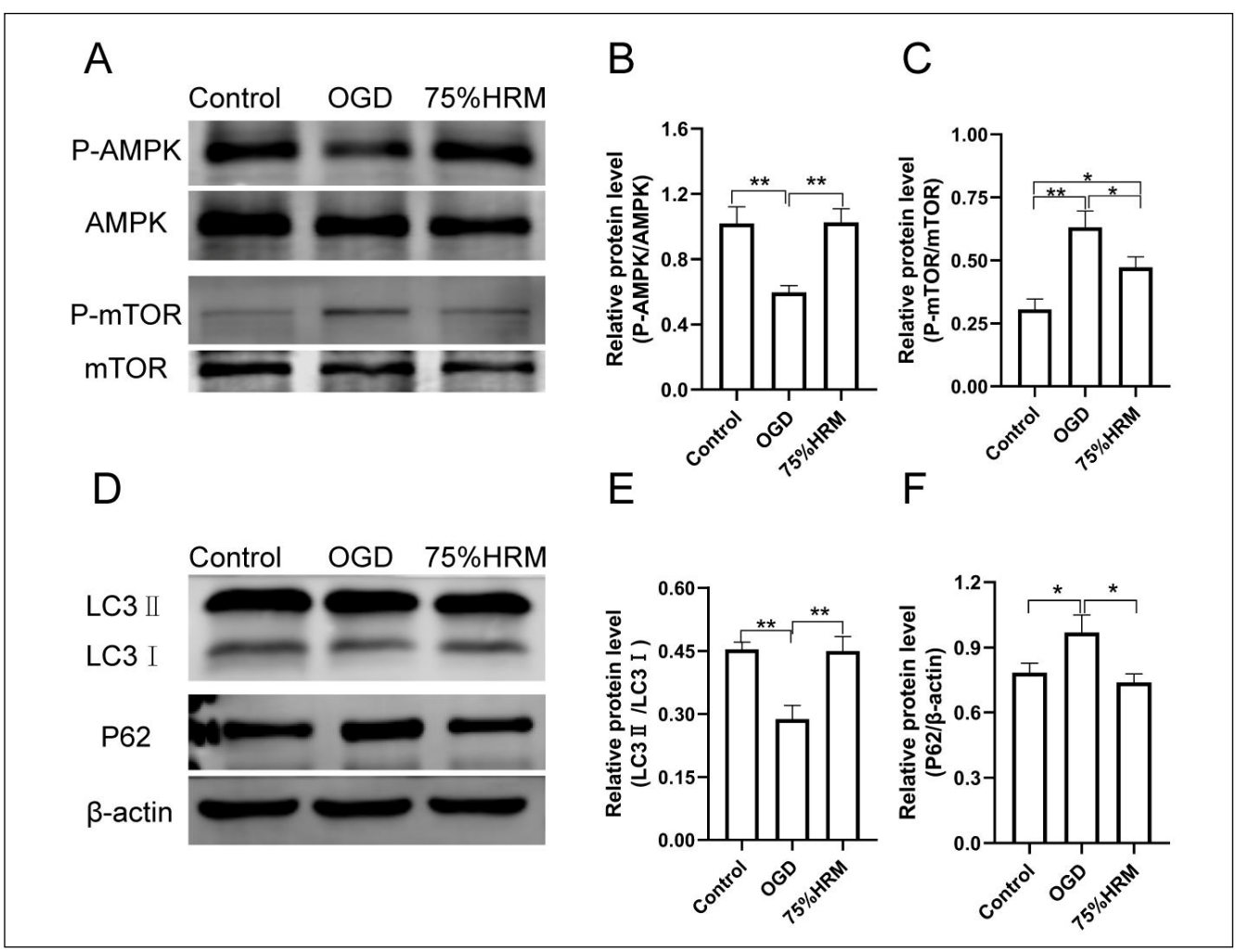

Fig. 6. HRM promoted AMPK phosphorylation and autophagy in PCNs after OGD. (A–C) The expression of p-AMPK, AMPK, p-mTOR and mTOR protein was detected by western blot. (D–F) The expression of LC3 and P62 protein was detected by western blot. *p<0.05, **p<0.01, ***p<0.001.

DISCUSSION

In the present study, we demonstrated that HRS improved neurological function in acute and long-term phases of ischemia. HRS alleviated oxidative stress and neuronal apoptosis and promoted synaptogenesis in dMCAO mice. Furthermore, we also found that HRM increased cell viability in PCNs treated with OGD and regulated AMPK/mTOR/autophagy signaling. These results suggest that HRS has a neuroprotective effect on cerebral ischemia by regulating AMPK/autophagy in ischemia mice.

Although hydrogen can be administered in several ways, such as inhalation of hydrogen gas, injection of HRS, oral hydrogen-rich water, and infiltration in a hydrogen-rich solution, a previous study demonstrated that the concentrations of hydrogen in the blood and organs were dependent on the dose and time, but not the method of administration by estimating the concentration of molecular hydrogen in pivotal organs (Song et al., 2015). Moreover, there is ample evidence suggesting that long-term hydrogen administration had no adverse effects on healthy animals by testing the biochemical parameters of organ-associated serum (Liu et al., 2014; Xun et al., 2020). Due to the safety and maneuverability of intraperitoneal injection, we selected it for administration and found that 20 ml/kg of HRS attenuated cerebral injury and neurological deficits induced by permanent ischemia in both acute- and chronic-term.

It was initially shown that hydrogen could protect I/R ischemia against oxidative stress by selectively scavenging detrimental reactive oxygen species, •OH and ONOO- (Ohsawa et al., 2007). Hydrogen has also been shown to be anti-inflammatory in neonatal hypoxic ischemia and adult ischemia by regulating the polarization of microglia (Huang et al., 2019; Chu et al., 2019). Moreover, hydrogen exerted an anti-apoptotic effect in a PC12 cell model of ischemia/reperfusion by stimulating Bcl-2. The evidence above suggests that hydrogen has a therapeutic effect on ischemia-reperfusion in animals via multiple mechanisms. In our study, we also found that HRS could induce a decrease in infarct volume and improve neurological function. Some preclinical studies and limited clinical trials suggest that hydrogen water may have neuroprotective properties. It is thought that the antioxidant and anti-inflammatory properties of hydrogen may help reduce oxidative stress and inflammation in the brain, which are commonly associated with neurodegenerative diseases and neuronal damage.

It is recognized that oxidative stress is involved in the pathophysiological cascade of cerebral ischemia, which leads to lipid peroxidation, mitochondrial and DNA damage, and antioxidant reserve depletion. At present, neutralization of oxidative stresses is a potential therapeutic target of pharmacological intervention after ischemia (Chamorro et al., 2016). Therefore, oxidative stress-related indicators, including SOD, GSH (indicators of antioxidant capacity) and MDA (indicators of oxidative damage), were detected to further explore the mechanism of HRS's therapeutic effect in the acute phase. Our study found that HRS administration increased SOD and GSH and decreased MDA, which was consistent with previous studies (Li et al., 2012; Zhao et al., 2015).

Previous studies have reported that ischemic-stroke-induced loss of dendritic spines in penumbra in vivo and in situ destroyed the integrity of neural connections and signal transmission pathways and led to sensorimotor deficits (Brown et al., 2008; Sigler and Murphy, 2010). It has been confirmed that endogenous repair of neural network remodeling contributes to long-term recovery after cerebral ischemia. We found that the HRS enhanced the spine population during the later chronic phase of cerebral ischemia in mice. PSD96 (a marker of postsynaptic membrane) and SYP (a marker of presynaptic membrane) can be representative of plasticity in dendrites and synapses. In the present study, the administration of HRS continuously was able to enhance the expression of PS95 and SYP. Moreover, the morphological results were consistent with behavioral findings; HRS promoted the recovery of neurological function in the late stage of cerebral ischemia. The experimental results indicated that long-term application of HRS can promote the formation of neural networks and improve the recovery of sensorimotor functions.

AMPK is a serine/threonine protein kinase that has been demonstrated to respond to energy metabolism, cell survival, apoptosis, and autophagy (Gong et al., 2021). Previous studies reported that AMPK exerted protective effects against global cerebral ischemia (Duan et al., 2019). The role of AMPK/mTOR signaling-mediated autophagy in cerebral ischemia remains controversial (Wang et al., 2019). Yang et al. (2021) reported that *Arctium lappa L.* roots ameliorated cerebral ischemia by suppressing AMPK/mTOR-mediated autophagy. A study by Wang et al. (2022) showed that EGCG inhibited autophagy through the AKT/AMPK/mTOR phosphorylation pathway and protected the mouse brain from cerebral ischemia/reperfusion injury. However, the study by L W et al. showed that eugenol attenuates cerebral ischemia-reperfusion injury by enhancing autophagy *via* the AMPK-mTOR-P70S6K pathway. A recent study showed that schaftoside improved cerebral ischemia-reperfusion injury by enhancing au-

tophagy through the AMPK/mTOR pathway (Zhang et al., 2022). Our results showed that HRS administration upregulated AMPK phosphorylation and downregulated mTOR phosphorylation, which led to the induction of autophagy. This finding was further verified by the observation of increased LC3 expression and decreased P62 expression. This conclusion was reached through in vitro experiments, and in-depth research on genetic material is needed in the future.

Our current study has some limitations. Multiple mechanisms are involved in cerebral ischemic stroke, and the impact of HRS on other signaling pathways is not well studied. Cerebral ischemia-reperfusion injury often occurs in stroke patients, and the impact of HRS on cerebral ischemia-reperfusion injury is still unclear. Whether HRS could promote the recovery of stroke patients through other mechanisms is our future focus. In addition to the above-mentioned AMPK/mTOR/autophagy signaling pathway, HRS may also regulate other signaling pathways to achieve its neuroprotective effect. For example, hydrogen has been shown to activate the Nrf2/ARE signaling pathway (Liu et al., 2019), which plays an important role in protecting cells from oxidative stress and inflammation. HRS may also regulate the JAK/STAT and PI3K/Akt/mTOR signaling pathways, which are important in regulating cell survival and proliferation. Further research is needed to explore the specific signaling pathways involved in the neuroprotective effect of HRS.

CONCLUSION

This study found that HRS had a protective effect on neurological function in mice with cerebral ischemia. HRS was found to decrease infarct volume and histological damage, decrease the number of apoptotic cells, enhance neuroplasticity, and promote neurological recovery. The mechanism of this protective effect may involve the autophagy pathway mediated by the AMPK/mTOR signaling pathway. These findings suggest that HRS may be a potential therapeutic agent for the treatment of cerebral ischemia.

REFERENCES

Bai X, Liu S, Yuan L, Xie Y, Li T, Wang L, Wang X, Zhang T, Qin S, Song G, Ge L, Wang Z (2016) Hydrogen-rich saline mediates neuroprotection through the regulation of endoplasmic reticulum stress and autophagy under hypoxia-ischemia neonatal brain injury in mice. Brain Res 1646: 410–417.

Brown CE, Wong C, Murphy TH (2008) Rapid morphologic plasticity of peri-infarct dendritic spines after focal ischemic stroke. Stroke 39: 1286–1291.

Chamorro Á, Dirnagl U, Urra X, Planas AM (2016) Neuroprotection in acute stroke: targeting excitotoxicity, oxidative and nitrosative stress, and inflammation. Lancet Neurol 15: 869–881.

Chu X, Cao L, Yu Z, Xin D, Li T, Ma W, Zhou X, Chen W, Liu D, Wang Z (2019) Hydrogen-rich saline promotes microglia M2 polarization and complement-mediated synapse loss to restore behavioral deficits following hypoxia-ischemic in neonatal mice via AMPK activation. J Neuroinflammation 16: 104.

Duan J, Cui J, Yang Z, Guo C, Cao J, Xi M, Weng Y, Yin Y, Wang Y, Wei G, Qiao B, Wen A (2019) Neuroprotective effect of Apelin 13 on ischemic stroke by activating AMPK/GSK-3β/Nrf2 signaling. J Neuroinflammation 16: 24.

Fu C, Wu Y, Liu S, Luo C, Lu Y, Liu M, Wang L, Zhang Y, Liu X (2022) Rehmannioside A improves cognitive impairment and alleviates ferroptosis via activating PI3K/AKT/Nrf2 and SLC7A11/GPX4 signaling pathway after ischemia. J Ethnopharmacol 289: 115021.

Gong S, Liu J, Wan S, Yang W, Zhang Y, Yu B, Li F, Kou J (2021) Schisandrol A attenuates myocardial ischemia/reperfusion-induced myocardial apoptosis through upregulation of 14-3-3θ. Oxid Med Cell Longev 2021: 5541753.

Huang JL, Liu WW, Manaenko A, Sun XJ, Mei QY, Hu Q (2019) Hydrogen inhibits microglial activation and regulates microglial phenotype in a mouse middle cerebral artery occlusion model. Med Gas Res 9: 127–132.

Joy MT, Carmichael ST (2021) Encouraging an excitable brain state: mechanisms of brain repair in stroke. Nat Rev Neurosci 22: 38–53.

Ke H, Liu D, Li T, Chu X, Xin D, Han M, Wang S, Wang Z (2020) Hydrogen-rich saline regulates microglial phagocytosis and restores behavioral deficits following hypoxia-ischemia injury in neonatal mice via the Akt pathway. Drug Design Develop Therapy 14: 3827–3839.

Li J, Dong Y, Chen H, Han H, Yu Y, Wang G, Zeng Y, Xie K (2012) Protective effects of hydrogen-rich saline in a rat model of permanent focal cerebral ischemia via reducing oxidative stress and inflammatory cytokines. Brain Res 1486: 103–111.

Liu C, Kurokawa R, Fujino M, Hirano S, Sato B, Li XK (2014) Estimation of the hydrogen concentration in rat tissue using an airtight tube following the administration of hydrogen via various routes. Sci Rep 4: 5485.

Liu Y, Dong F, Guo R, Zhang Y, Qu X, Wu X, Yao R (2019) Hydrogen-rich saline ameliorates experimental autoimmune encephalomyelitis in C57BL/6 mice via the Nrf2-ARE signaling pathway. Inflammation 42: 586–597.

Llovera G, Roth S, Plesnila N, Veltkamp R, Liesz A (2014) Modeling stroke in mice: permanent coagulation of the distal middle cerebral artery. JoVE 89: e51729.

Mo XY, Li XM, She CS, Lu XQ, Xiao CG, Wang SH, Huang GQ (2019) Hydrogen-rich saline protects rat from oxygen glucose deprivation and reperusion-induced apoptosis through VDAC1 via Bcl-2. Brain Res 1706: 110–115.

Moujalled D, Strasser A, Liddell JR (2021) Molecular mechanisms of cell death in neurological diseases. Cell Death Differ 28: 2029–2044.

Ohsawa I, Ishikawa M, Takahashi K, Watanabe M, Nishimaki K, Yamagata K, Katsura K, Katayama Y, Asoh S, Ohta S (2007) Hydrogen acts as a therapeutic antioxidant by selectively reducing cytotoxic oxygen radicals. Nature Med. 13: 688–694.

Ono H, Nishijima Y, Adachi N, Tachibana S, Chitoku S, Mukaihara S, Sakamoto M, Kudo Y, Nakazawa J, Kaneko K, Nawashiro H (2011) Improved brain MRI indices in the acute brain stem infarct sites treated with hydroxyl radical scavengers, Edaravone and hydrogen, as compared to Edaravone alone. A non-controlled study. Medical Gas Res 1: 12.

Ono H, Nishijima Y, Ohta S, Sakamoto M, Kinone K, Horikosi T, Tamaki M, Takeshita H, Futatuki T, Ohishi W, Ishiguro T, Okamoto S, Ishii S, Takanami H (2017) Hydrogen gas inhalation treatment in acute cerebral infarction: A randomized controlled clinical study on safety and neuroprotection. J Stroke Cerebrovasc Dis 26: 2587–2594.

Sennfält S, Pihlsgard M, Norrving B, Ullberg, T, Petersson J (2021) Ischemic stroke patients with prestroke dependency: Characteristics and long-term prognosis. Acta Neurol Scand 143: 78–88.

Sigler A, Murphy TH (2010) In vivo 2-photon imaging of fine structure in the rodent brain: before, during, and after stroke. Stroke 41: S117–S123.

Song G, Zong C, Zhang Z, Yu Y, Yao S, Jiao P, Tian H, Zhai L, Zhao H, Tian S, Zhang X, Wu Y, Sun X, Qin S (2015) Molecular hydrogen stabilizes atherosclerotic plaque in low-density lipoprotein receptor-knockout mice. Free Rad Biol Med 87: 58–68.

van der Worp HB, Macleod MR, Bath PM, Bathula R, Christensen H, Colam B, Cordonnier C, Demotes-Mainard J, Durand-Zaleski I, Gluud C, Jakobsen JC, Kallmünzer B, Kollmar R, Krieger DW, Lees KR, Michalski D, Molina C, Montaner J, Roine RO, Petersson J, EuroHYP-1 investigators (2019) Therapeutic hypothermia for acute ischaemic stroke. Results of a European multicentre, randomised, phase III clinical trial. Eur Stroke J 4: 254–262.

Wang G, Wang T, Zhang Y, Li F, Yu B, Ko J (2019) Schizandrin protects against OGD/R-induced neuronal injury by suppressing autophagy: Involvement of the AMPK/mTOR pathway. Molecules 24: 3624.

Wang L, Dai M, Ge Y, Chen J, Wang C, Yao C, Lin Y (2022) EGCG protects the mouse brain against cerebral ischemia/reperfusion injury by suppressing autophagy via the AKT/AMPK/mTOR phosphorylation pathway. Front Pharmacol 13: 921394.

Wang P, Zhao M, Chen Z, Wu G, Fujino M, Zhang C, Zhou W, Zhao M, Hirano SI, Li XK, Zhao L (2020) Hydrogen gas attenuates hypoxic-ischemic brain injury via regulation of the MAPK/HO-1/PGC-1a pathway in neonatal rats. Oxid Med Cell Longev 2020: 6978784.

Williamson MR, Franzen RL, Fuertes CJA, Dunn AK, Drew MR, Jones TA (2020) A window of vascular plasticity coupled to behavioral recovery after stroke. J Neurosci 40: 7651–7667.

Xu SY, Wu YM, Ji Z, Gao XY, Pan SY (2012) A modified technique for culturing primary fetal rat cortical neurons. J Biomed Biotechnol 2012: 803930.

Xu W, Li K, Fan Q, Zong B, Han L (2020) Knockdown of long non-coding RNA SOX21-AS1 attenuates amyloid-β-induced neuronal damage by sponging miR-107. Biosci Rep 40: BSR20194295.

Xue J, Yu Y, Zhang X, Zhang C, Zhao Y, Liu B, Zhang L, Wang L, Chen R, Gao X, Jiao P, Song G, Jiang XC, Qin S (2019) Sphingomyelin synthase 2 inhibition ameliorates cerebral ischemic reperfusion injury through reducing the recruitment of toll-like receptor 4 to lipid rafts. J Amn Heart Assoc 8: e012885.

Xun ZM, Zhao QH, Zhang Y, Ju FD, He J, Yao TT, Zhang XK, Yi Y, Ma SN, Zhao PX, Jin XY, Li YX, Li XY, Ma XM, Xie F (2020) Effects of long-term hydrogen intervention on the physiological function of rats. Sci Rep 10: 18509.

Yan W, Sun W, Fan J, Wang H, Han S, Li J, Yin Y (2020) Sirt1-ROS-TRAF6 signaling-induced pyroptosis contributes to early injury in ischemic mice. Neurosci Bull 36: 845–859.

Yang Y, Gao H, Liu W, Liu X, Jiang X, Li X, Wu Q, Xu Z, Zhao Q (2021) Arctium lappa L. roots ameliorates cerebral ischemia through inhibiting neuronal apoptosis and suppressing AMPK/mTOR-mediated autophagy. Int J Phytother Phytopharmacol 85: 153526.

Yousefifard M, Shamseddin J, Babahajian A, Sarveazad A (2020) Efficacy of adipose derived stem cells on functional and neurological improvement following ischemic stroke: a systematic review and meta-analysis. BMC Neurol 20: 294.

Zhang K, Zhang Q, Deng J, Li J, Li J, Wen L, Ma J, Li C (2019) ALK5 signaling pathway mediates neurogenesis and functional recovery after cerebral ischemia/reperfusion in rats via Gadd45b. Cell Death Dis 10: 360.

Zhang L, Wu M, Chen Z (2022) Schaftoside improves cerebral ischemia-reperfusion injury by enhancing autophagy and reducing apoptosis and inflammation through the AMPK/mTOR pathway. Adv Clin Exp Med 31: 1343–1354.

Zhang P, Zhang X, Huang Y, Chen J, Shang W, Shi G, Zhang L, Zhang C, Chen R (2021) Atorvastatin alleviates microglia-mediated neuroinflammation via modulating the microbial composition and the intestinal barrier function in ischemic stroke mice. Free Rad Biol Med 162: 104–117.

Zhao L, Chen X, Dai Q, Zhang L, Yu P, Gao Y, Wu L, Duan M, Xu J (2015) [Role of FOXO3a in process of hydrogen-rich saline attenuating global cerebral ischemia-reperfusion injury in rats]. Zhonghua yi xue za zhi 95: 457–461.

SUPPLEMENTARY MATERIALS

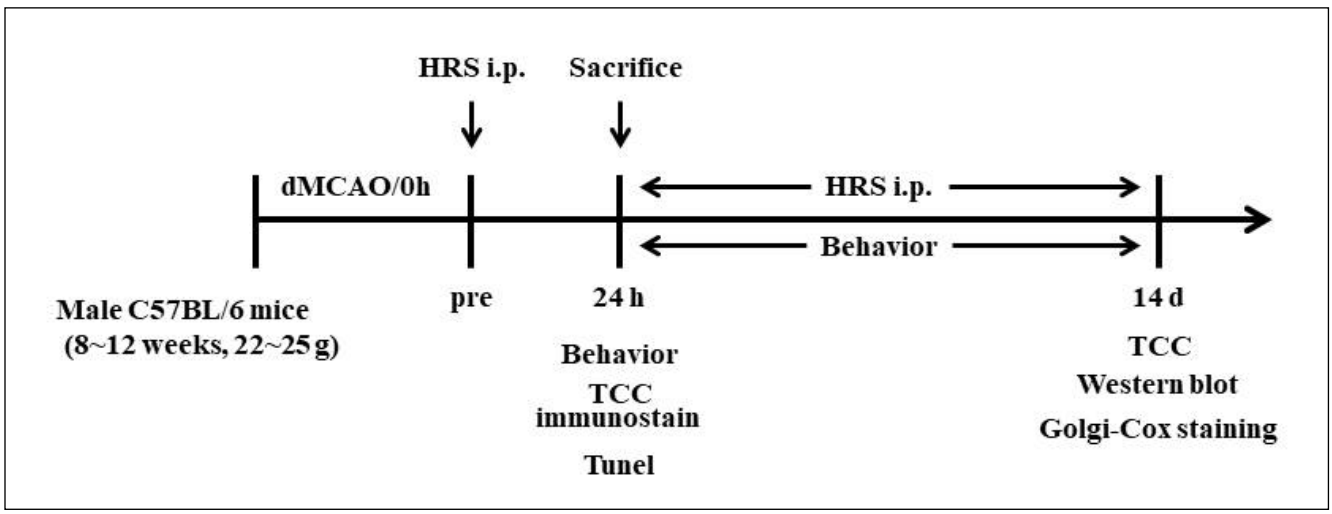

Additional Flowchart